CAMBRIDGE
UNIVERSITY PRESS

RESEARCH ARTICLE

Topological relation expression and verification of symmetrical parallel mechanism based on the evolution of chemical molecule

Litao He[1,3], Hairong Fang[1] (ID) and Dan Zhang[2,3]

[1]Department of Mechanical Engineering, Beijing Jiaotong University, Beijing, PR China, [2]Department of Mechanical Engineering, The Hong Kong Polytechnic University, Hong Kong, China, and [3]Department of Mechanical Engineering, Lassonde School of Engineering, York University, Toronto, Canada
Corresponding author: Hairong Fang; Email: hrfang@bjtu.edu.cn

Abstract

The research of parallel mechanism (PM) configuration involves many problems. From topology to configuration, dimensional constraint, etc., how to establish the relationship between topology and configuration with effective methods is a long-term challenge for the configuration design. In this paper, the chemical molecular spatial structure (CMSS) is linked with the configuration of symmetrical parallel mechanism (SPM). Starting from the methane molecule (CH_4), a spatial structural topological relation is obtained. Based on graph theory and the spatial structural topological relation, a new expression method with topological graph and its kinematic pair adjacency matrix for spatial SPM is proposed. Then, the expression and analysis for the characteristics of spatial SPM are obtained. Finally, by taking the 3-RPS PM and the 3-RRC PM as examples, the effectiveness and corresponding consistency of the proposed expression method are successfully verified. The proposed new expression method paves the way for the subsequent digital and automated design and analysis of the SPM configuration.

1. Introduction

Due to the difference in microstructure and composition of molecular spatial structure, chemical substances can go deep into various fields with different practicability. In the design of mechanism configuration, the essence is also due to the difference in structure and composition. Therefore, whether it is macroscopic or microscopic, the structure determines its properties [1].

In chemistry, the spatial configuration of a molecule [2] reflects the distribution of various atoms. These atoms are combined to form a whole molecule based on certain rules. Hence, a certain geometric shape in space can be presented by the molecular structure. Some common CMSSs, such as V-shaped, straight-line-shaped, triangular cone-shaped, and regular tetrahedral-shaped [3], etc., their structures, are shown in Fig. 1.

Among many spatial molecular configurations, the most representative molecular structure is the regular tetrahedron. As shown in Fig. 2, the regular tetrahedron is a stable three-dimensional structure, which is the basic component of all spatial polyhedrons. Methane molecule (CH_4) and white phosphorus molecule (P_4) belong to the common regular tetrahedral structure of chemical molecules. Their spatial structures are shown in Fig. 3. CH_4 is an organic compound, and its chemical properties are relatively stable [4], while the chemical properties of P_4 are very active and unstable. Although the two chemical molecules are both regular tetrahedral structures, their properties are quite different due to the different atomic types and chemical bonds in space.

Chemical molecules are usually expressed in many forms. With the appearance of molecular structural formula, the spatial structural relationship of chemical molecule is transformed into a planar
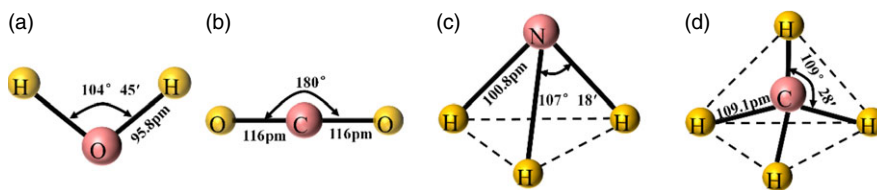
Figure 1. *Spatial configuration of different molecules. (a) V-shaped. (b) Straight-line-shaped. (c) Triangular cone-shaped. (d) Regular tetrahedral-shaped.*
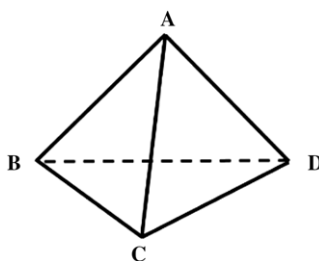

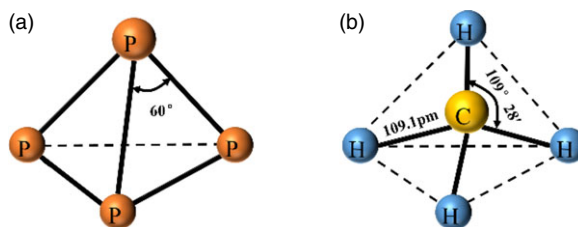**Figure 2.** *Spatial regular tetrahedron structure.*

Figure 3. *Chemical molecules with regular tetrahedral structure. (a) P_4. (b) CH_4.*
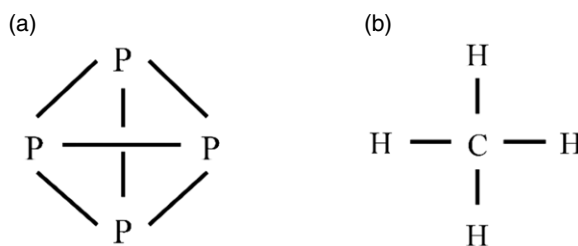

Figure 4. *Structural formula of chemical molecules. (a) Structural formula of P_4. (b) Structural formula of CH_4.*

connection relationship. Element symbols and short lines are used to represent the arrangement and combination of atoms in molecules [2]. Then, the expression of molecular spatial structure is further simplified. For example, the planar structural formulas are shown in Fig. 4, and the spatial structures of P_4 and CH_4 are significantly simplified. Hence, with the corresponding relationship between CMSS and planar structural formula, it is shown that the spatial structure also can be described in the form of a planar connection relationship.

In summary, the spatial structure can be expressed as a corresponding planar topological connection relationship. However, in the research of mechanisms, there are various forms of mechanisms, including planar mechanisms, spatial mechanisms, cam mechanisms, gear mechanisms, etc. The topological method is proposed by graph theory based on non-logical thinking. Although the topological method

can be used to design the topological structure of mechanisms [5, 6], it usually only represents the topological relationship of planar linkage mechanisms. For other types of mechanisms, such as mechanisms with compound hinges and spatial multi-link mechanisms, etc., scholars also have proposed some corresponding topological models [7–12]. Nevertheless, these models are more complicated, and they are not conducive to establishing the relationship with various mechanisms. Of course, for the spatial PM, the expression in the form of topological graph is almost blank. It is still a long-term challenge for the configuration design of PMs to establish the expression of topology and configuration with effective methods, and simplify the analysis.

On the other hand, for the structural characteristics of spatial PMs, such as many spatial SPMs with structures of regular tetrahedron [13, 14] and regular polyhedron [15], the current descriptions are mostly expressed by mechanism diagrams. In the process of drawing diagrams, the representation of the kinematic pair relationship for mechanism is complicated. At this stage, there are few relevant studies on expressing the topological relationship of spatial PMs with graph theory. However, the construction of topological relations in mechanism innovation is an important basis for generating new mechanisms [16–18]. By using graph theory, the expression for topological relations of spatial PMs is more concise and intuitive, and it is convenient to use mathematical methods for analysis. What's more, the topological expression is more conducive to discovering new mechanisms. Of course, for spatial PMs, the application of graph theory is also limited. Since there are many similarities in essence between chemical molecular structure and mechanism configuration, the chemical molecular structure can be transformed from spatial structure to planar connection relationship. Moreover, graph theory is often used to express the topological connection relationship of mechanisms. Therefore, in order to further explore the relationship between chemical molecular structure and spatial mechanism configuration, and to relieve the limitation that the general graph theory method can only design planar mechanisms, this paper is started from the perspective of CMSS, combined with the graph theory method, to develop the related research on spatial mechanism configuration.

In this paper, based on the most representative regular tetrahedral structure of the chemical molecule CH_4 in space and its stable spatial structural characteristics, the spatial regular tetrahedral structure of CH_4 is evolved into a planar topological relationship. The spatial stable configuration of CH_4 is expressed in the form of a topological graph, and it is shown that the correlation of design between spatial stable structure and planar topological structure. Hence, the topological graph of spatial configuration is extended and applied to express the topological relationship of spatial PM. The structure of this paper is organized as follows: Section 2 uses the spatial regular tetrahedral structure of CH_4 for topological evolution and obtains the topological graph of the molecular spatial stable structure. According to the obtained topological relationship, a new topological expression method of spatial SPM is proposed and described in Section 3. Section 4 verifies the proposed topological graph and mathematical analysis method of the spatial SPM. An example for digital and automated design based on topological graph is given to explain the design method in Section 5. Finally, the conclusions are drawn in Section 6.

2. Topological evolution with the spatial regular tetrahedral structure of CH_4

2.1. Introduction to the spatial structure of CH_4

In the chemical molecular structure, when an atom interacts with other four identical atoms, four chemical bonds can be formed. If each bond has the same bond length and bond angle, the spatial regular tetrahedral structure is formed. For example, methane molecule (CH_4), carbon tetrachloride molecule (CCl_4), etc., all belong to the spatial regular tetrahedral molecular configuration. Conversely, if there is a different bond parameter, it will belong to the spatial tetrahedral structure, such as monochloromethane molecule (CH_3Cl), trichloromethane molecule ($CHCl_3$), etc.

The regular tetrahedral structure of chemical molecules have a stable existence of three-dimensional structure compared to other spatial structure molecules. Its properties are more stable, and its structure is simpler. CH_4 is the most representative molecule among the regular tetrahedral structure chemical
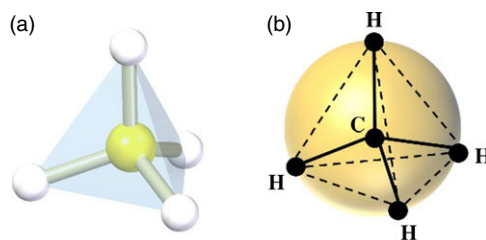
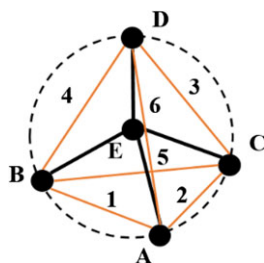**Figure 5.** *Structure of CH$_4$. (a) 3D model. (b) Spatial structure.*

Figure 6. *The spatial regular tetrahedral structure of CH$_4$.*

molecules, so this paper is based on CH$_4$ molecule to perform the topological evolution of the spatial structure.

The spatial regular tetrahedral structure of CH$_4$ [19] is shown in Fig. 5. It includes four identical C-H bonds with bond lengths of 109.1pm and bond angles of 109°28′ [3]. The molecular structure is a spatial symmetrical structure, and it exists in a stable state for a long time.

The properties of substances are the external performance of the molecular structure. In the formation of CH$_4$, due to the interaction between C atom and H atoms, each bond is formed with the same length and angle. Hence, a spatial regular tetrahedral molecule is obtained. In addition, the C atom of CH$_4$ is located in the center of regular tetrahedron structure, and the distance from C atom to each vertex is the C-H bond length. It can be described mathematically that each vertex of the regular tetrahedron structure of CH$_4$ is distributed on its circumscribed sphere, and the radius of the circumscribed sphere is the bond length.

To obtain mechanisms with stronger spatial structural stability, the spatial symmetrical molecular structure is used as the prototype in this paper, and the evolution from spatial structure to planar topology will be deduced.

2.2. Topological evolution for the spatial structure of CH$_4$

After describing the spatial structure characteristics of CH$_4$ in Section 2.1, the evolution of molecular configuration is deduced in this section. As shown in Fig. 6, it is the spatial regular tetrahedral structure of CH$_4$. The connection relationship between various element points for the spatial configuration of the chemical molecule is retained, and the spatial characteristics for the circumscribed circle of molecular structure are also reflected.

Due to the intersection of multiple edges in a regular tetrahedron, the description of the spatial geometric relationship is complex. Thus, it is necessary to simplify the main geometric feature information and express the spatial connection relationship of each element clearly. The expression of edges and vertex positions for constituting the tetrahedral structure needed to be reduced. In the process of evolution, since the information of the four vertices of regular tetrahedron structure is known, the four structural
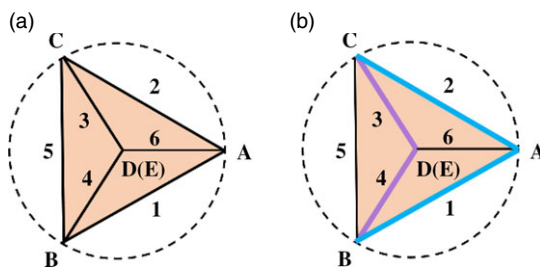
Figure 7. *Top view and projection edges of the regular tetrahedral structure. (a) Top view. (b) Four projection edges.*
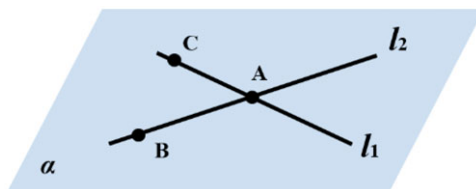

Figure 8. *Two intersecting lines in space.*

edges of AB, AC, BD, and CD are used to express the spatial structure. The four structural edges are transformed from spatial structure into planar graph to express the basic configuration characteristics of the regular tetrahedral structure, and the reasons are as follows:

By projecting the regular tetrahedral structure onto plane, the top view is obtained, as shown in Fig. 7(a). According to the structural characteristics, it is necessary to determine any surface as the bottom surface of the regular tetrahedron firstly. Here, assuming that the bottom of the regular tetrahedron is △ABC, then three vertex information of the regular tetrahedron structure is expressed, and the bottom △ABC of the regular tetrahedron just can be determined by the edge AB and AC, as shown in Fig. 7(b). Secondly, on the basis of the determined bottom △ABC, it is also necessary to express the edge and vertex height information of regular tetrahedron structure. As shown in Fig. 7(b), the above information can be determined by the edge BD and CD. To sum up, the spatial feature information of regular tetrahedron structure is determined by these four edges, so they can be used to simplify the expression of the regular tetrahedron structure on the plane.

It is known that two straight lines l_1 and l_2 in space intersect at point A, as shown in Fig. 8. Thus, it is necessary to prove that there is only one plane α passing through the straight lines l_1 and l_2, that is, the bottom surface of the above regular tetrahedron.

As shown in Fig. 8, taking another point C that does not coincide with A on the straight line l_1, and then taking another point B that does not coincide with A on the straight line l_2, it can be obtained that the three points A, B, and C are not collinear.

According to axiom three [20] in space solid geometry, it can be known that there is one and only one plane passing through three points that are not on a straight line. Hence, there is one and only one plane α through points A, B, and C.

On the contrary, according to the axiom one [20] in space solid geometry, it can be known that if two points on a straight line are in a plane, then all the points on the straight line are in this plane.

Since A∈α, B∈α, we can get: $l_2 \subset α$, and $l_1 \subset α$.

Thus, through two intersecting straight lines l_1 and l_2, there is one and only one plane α.

That is, two intersecting lines determine a plane.

Therefore, as shown in Fig. 9, the position of the bottom surface △ABC of regular tetrahedron structure can be determined by using the edges AB and AC. The proposed edges are proved.
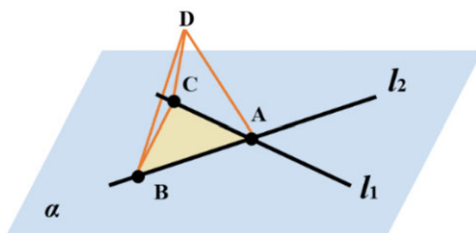
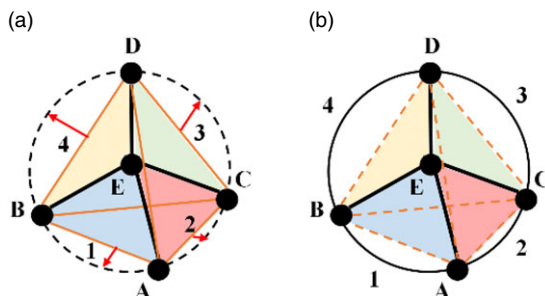**Figure 9.** *The bottom surface of regular tetrahedron.*

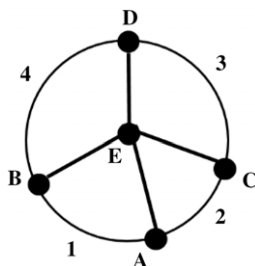**Figure 10.** *Evolution of edges. (a) Evolution of four edges. (b) Planar topological expression.*

Figure 11. *Preliminary topological graph for the spatial structure of CH_4.*

It can be seen from the above analysis that the two edges AB and AC intersect, so it is shown that the points A, B, and C are coplanar, that is, the bottom surface of spatial regular tetrahedron structure is determined. When the three points A, B, and C are known, the information for the bottom surface of the regular tetrahedron structure can be expressed by the two edges AB and AC. In the same way, it can be proved that the two intersected edges BD and CD determine the plane, where $\triangle BCD$ is located. Then, the information for the vertex and high of spatial regular tetrahedron structure is determined. Hence, the four edges AB, AC, BD, and CD of the spatial regular tetrahedron structure can be used to express its characteristics. It is further shown that the edges selected in this section can be used to evolve and represent the spatial characteristics of regular tetrahedron structure.

In the process of evolution, to facilitate the distinction and analysis, the spatial tetrahedral structural features are decomposed into multiple triangles. The edges AB, AC, BD, and CD correspond to $\angle AEB$, $\angle AEC$, $\angle BED$, and $\angle CED$, respectively, as shown in Fig. 10(a). After the four edges of the structure are transformed into the circumcircle of the regular tetrahedron, the planar topological expression is generated as shown in Fig. 10(b).

Then, the redundant lines and color expressions are removed, and a preliminary topological graph for the spatial structure of CH_4 is obtained, as shown in Fig. 11. Among them, the core skeleton of CH_4 is retained, and the molecular spatial topological structure is simplified to the plane.
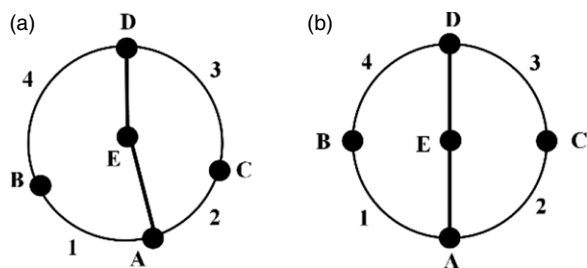
Figure 12. *Topological graph for the spatial structure of CH₄. (a) The simplified graph. (b) The final topological graph.*
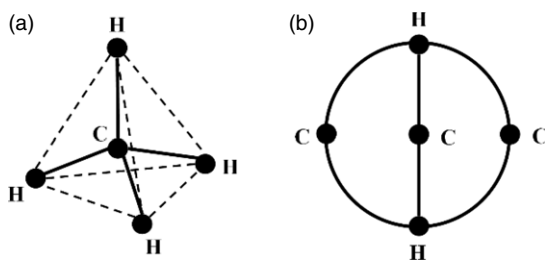

Figure 13. *The spatial structure and topological graph of CH₄. (a) Spatial structure. (b) Topological graph.*

During the evolution of the above molecular spatial structure, the edge AB of △ABE, the edge AC of △ACE, the edge BD of △BDE, and the edge CD of △CDE have all been evolved to the circum-circle. And in the evolution of △ABE and △ACE, △BDE, and △CDE, there are two common edges AE and DE; that is, the other edge feature of the above triangle is also expressed. Based on the above information, each triangle in the molecular spatial structure is expressed with the existing topological relationship. Then, the redundant connection relationship can be removed, and the connection between B, C, and E is further simplified. Thus, the topological graph based on the molecular spatial structure is obtained, as shown in Fig. 12(a). On the other hand, since the expressions of two common edges AE and DE have already existed in △AED, the connection relationship is preserved. By sorting out, the final topological graph for the molecular spatial structure of regular tetrahedral is obtained, as shown in Fig. 12(b).

2.3. Topological evolution results for the spatial structure of CH₄

After the evolution of the topological relationship in Section 2.2, the spatial regular tetrahedral structure of CH₄ has been expressed with the planar topological relationship, as shown in Fig. 13. It is a more simplified form to describe the spatial structure.

Based on the molecular spatial structure of CH₄, as shown in Fig. 13(a), C is at the center of the molecular structure and H is at the two ends of each branch of the regular tetrahedral structure, that is: C is in the middle of each H-C-H branch, and C belongs to the common connecting part. Therefore, the topological connection form of H-C-H that exists in CH₄ is still preserved during the evolution process. Also, due to the symmetric form of the spatial regular tetrahedral structure, the structure of each branch is the same and can be completely overlapped by rotation, so it can be simplified to be one branch chain structure to analyze. And the shape of the external sphere of CH₄ spatial structure is preserved in the evolution process, so the topological graph is in a circular form. In this paper, by using such a connection
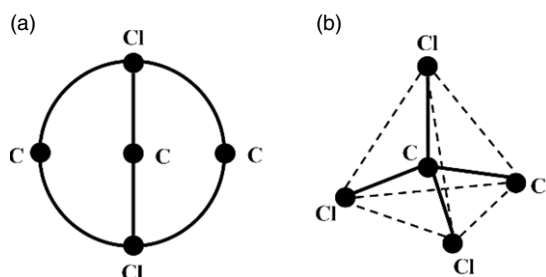
Figure 14. *The carbon tetrachloride molecule. (a) Topological graph. (b) Spatial structure.*

relationship in the spatial structure of CH_4 for topological evolution expression, the elements in each branch are split and merged based on the expression form of shared connection, so the topological graph of the spatial structure as shown in Fig. 13(b) is obtained.

Through analyzing the topological graph of CH_4, it can be concluded that the left, middle, and right branches of the topological graph are exactly the same. The C atom of each branch is taken as the core, and it connects two H atoms up and down to generate two C-H bonds. The H atoms at the top and bottom of the topological graph are shared, so as to form three branches, and then, the topological relationship for the spatial structure of CH_4 is expressed.

Similarly, using the same topological expression form of CH_4, if the C-H bond is replaced by the C-Cl bond, a carbon tetrachloride molecule (CCl_4) is formed. Its topological graph is shown in Fig. 14(a), and the corresponding spatial structure is shown in Fig. 14(b); that is, it is also a spatial regular tetrahedron structure.

By comparing the topological graph and spatial structure of CH_4 and CCl_4, it can be found that: for the same type of CMSS, the element symbols in topological graphs are different, and the chemical bonds formed are different, so the types and properties of chemical molecules are different, but the expressions of topological graphs are the same; that is, the number of branches, the number of elements, and the connection relationship are the same. Hence, the same type of chemical molecular spatial structure can be expressed in the form of the same topological graph. It is distinguished by labeling element symbols, and the topological relationship expression for a class of chemical molecules with the same structure can be obtained.

From the above analysis results, it is shown that the topological graph can be used to express the structure and element connection relationship of molecular spatial structure. The chemical bonds between atoms are used to form a stable spatial structure. For the mechanism, a spatial mechanism is formed through the kinematic pairs between components. The kinematic pairs play the same role as the chemical bonds in spatial structure. Thus, the chemical molecular structure and mechanism configuration can be analogized in the evolution. For example, the CMSS is expressed by the topological graph, and different chemical molecules under the same spatial structure are obtained by replacing chemical bonds. These methods can be further applied to the expression of spatial mechanisms. A similar form of the topological graph for molecular structure can be used to express spatial PMs. By changing the types of kinematic pairs between components in the topological graph, different PM configurations are generated, and the configuration design and expression of the same type of mechanism can be realized.

To sum up, combined with the expression of topological graph for CMSS and the graph theory method of planar topological structure, the two are introduced into the expression of topological relationship of the spatial PM. Hence, a new topological method is used to represent PM, simplify the expression, and establish the connection between PMs and topological models. The new topological graph method is to relieve the limitation of the application of graph theory and realize the research goal of mechanism configuration design.
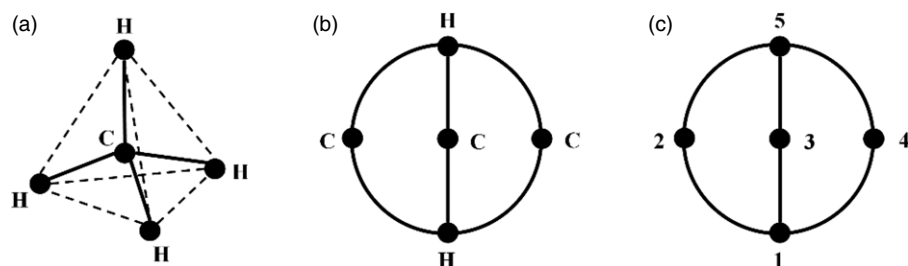
Figure 15. *The spatial topological structure of CH$_4$. (a) Spatial structure. (b) Topological graph. (c) Topological graph prototype.*

3. New topological expression method for spatial SPM

3.1. Topological evolution results for the spatial structure of CH$_4$

Through the topological transformation of molecular spatial structure, the above evolution results show that the spatial structure and planar topological graph can be effectively transformed. Hence, researching the relationship between spatial structure and topological graph helps to generate new spatial configurations quickly.
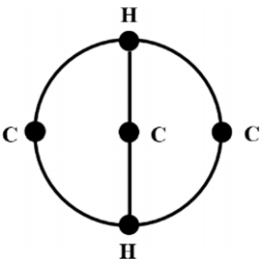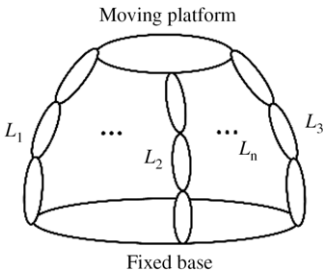
The spatial topological structure of CH$_4$ shown in Fig. 15 is analyzed, and it has the following characteristics:

1. Since the molecular structure of CH$_4$ belongs to a spatial symmetrical structure, the evolution retains this feature. Thus, the topological graph is still symmetrical, that is, the three branches are exactly the same, and can be overlapped by rotation.

2. The expression of spatial structure is simplified by the topological graph, but its characteristics are still retained, that is, the element arrangement of branches in the topological graph is the same as molecular spatial structural characteristics, and the corresponding relationship is consistent.

3. In each closed-loop triangle of the spatial structure, the C atom is taken as the center, and two H atoms are connected to form each branch. The regular tetrahedral structure is formed by three branches. The same characteristics are still in the corresponding topological graph, and the chemical bond is represented by a solid line.

4. The common elements and chemical bonds in the spatial structure are merged and split in the topological graph. The branch distribution is simplified in these ways.

5. The shape of the topological graph is obtained from the evolution of the circumscribed sphere of spatial regular tetrahedron structure, so the shape of the topological graph is round. The spatial structure can be better represented by this feature of a round.

PM has many configurations, and each configuration has multiple chains. Considering that the spatial structure of CH$_4$ is symmetrical. Thus, the topological graph of CH$_4$ is compared with the structure of the symmetrical parallel mechanism (SPM). There are many similarities between them, as shown in Table I.

It can be seen from Table I that the spatial structural topological graph of CH$_4$ is very similar to the structural characteristics of SPM. They are both composed of upper parts, lower parts, and multiple branches, and the branches in their respective structures are the same. They both have multiple spatial closed-loop chains. SPM is composed of multiple branch chains with the same structural form, and branch chains are connected to the moving platform and the fixed platform through kinematic pair. These branch chains are evenly distributed, and each branch chain can coincide after rotation, so it belongs to the spatial symmetrical mechanism. In fact, the spatial structural topological graph of CH$_4$ is exactly the same expression form. Therefore, in the expression of the topological relationship of spatial

Table I. *Comparison for topological graph of CH_4 and SPM.*

	Expression form	Structural features	Branch characteristics	Meaning
Topological graph of CH_4		1. Two vertices 2. Multiple branches	Contains multiple chemical elements and chemical bonds	Expressing the topological relationship of spatial structure
Brief diagram of SPM		1. Two platforms 2. Multiple branches	Contains multiple components and kinematic pairs	Expressing the relative motion relationship between the components of mechanism

mechanism, SPM is taken as the research object. It is combined with the spatial structural topological graph of CH_4, the topological relationship of SPM is described, and the configuration information of SPM is expressed, so as to realize the configuration analysis and design of SPM.
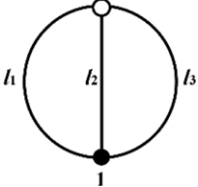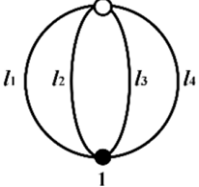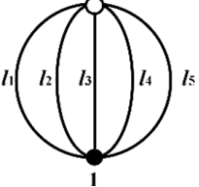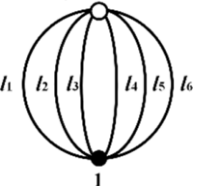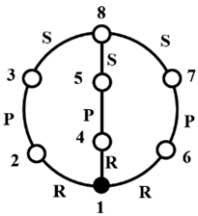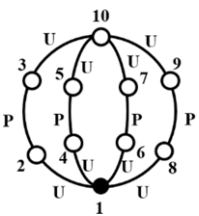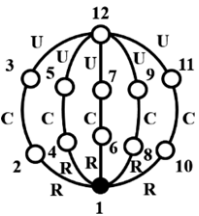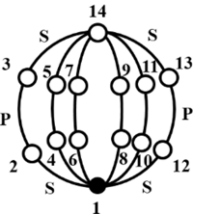
3.2. Definition for the topological graph of spatial SPM

A graph is a collection of vertices or nodes connected together by lines or edges. In the topological graph of planar mechanism, the components are represented by points and the kinematic pairs are represented by edges [21]. The topological graph has a certain corresponding relationship with the structural diagram of the planar mechanism. According to the basic definition of the graph, combined with the spatial structural topological graph of CH_4 and the representing method of planar mechanism, the topological graph of spatial SPM is defined as follows:

Assuming that the spatial SPM is Ms. For the mechanism Ms, the number of branch chains of Ms is m, and the number of kinematic pairs of each branch is k. Then, the number of vertices of the topological graph is $n = m \cdot (k - 1)$, and the number of edges of the topological graph is $e = m \cdot k$. To facilitate the analysis, each component and kinematic pair are uniformly numbered here. It is stipulated that the fixed platform serial number is set as 1, and the moving platform serial number is set as n. The components and kinematic pairs of each branch chain are numbered sequentially from left to right and from bottom to top (from the fixed platform to the moving platform). Similarly, the components are also represented by circles (in which the hollow circle represents the movable component, the solid circle represents the fixed component), and the kinematic pairs are represented by edges. At the same time, in order to reflect the feature of the spatial structure, the circular contour is still adopted in the topological graph, and thus the topological graph of the mechanism Ms is obtained.

According to the above definition of the topological graph of SPM, the expression form of the topological graph for spatial SPM can be obtained, as shown in Fig. 16. The unified form of spatial SPM is

Table II. *Types of topological graph for spatial SPMs.*

Spatial SPM	3-branch chains	4-branch chains	5-branch chains	6-branch chains
Expression form				
m	3	4	5	6
k	3	3	3	3
n	8	10	12	14
DOF	3	4	5	6
Kinematic pair	R, P, S	U, P, U	R, C, U	S, P, S
Topological graph				
Represented mechanism	3-RPS PM	4-UPU PM	5-RCU PM	6-SPS PM
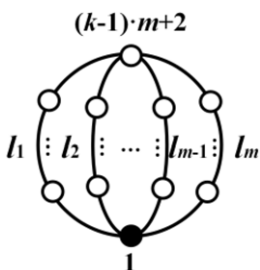
Figure 16. *Topological graph of spatial SPM.*

represented by this topological graph, that is, the topological graph of spatial SPM with m branch chains, and each branch chain contains k kinematic pairs. Meanwhile, from the characteristics of the spatially symmetric parallel mechanism, it is known that the DOF of the spatially symmetric parallel mechanism is equal to the number of branch chains of the mechanism topological graph, that is, the DOF is m.

From the definition of graph theory and the topological graph of SPM, it can be known that: for all spatial SPMs with m branch chains and the number of kinematic pairs of each branch chain is k, the corresponding topological graphs are isomorphic graphs. Namely, the topological graph has the same structural form, and the same kind of SPM can be represented by any one of the topological graphs. Hence, by sorting out and giving examples of the structural types of the topological graph for spatial SPM, as shown in Table II, the topological graph of SPM with three to six branch chains can be obtained.

3.3. *Mathematical expression and properties of the topological graph*

After transforming the spatial SPM to a topological graph, to facilitate subsequent automatic processing and analysis by computer [22], it is necessary to express the topological graph of SPM in a mathematical form and describe the topological relationship. Since the matrix is an effective mathematical tool to study graph theory, and the general adjacency matrix and the correlation matrix [23, 24] can describe all topological characteristics of the topological graph. Hence, the adjacency matrix is taken as the algebraic representation of topological graph for configuration design and analysis in this paper. However, the general adjacency matrix only expresses the connection relationship between components. The mechanism topology information is described less, and the correspondence between the matrix and configuration is poor. Therefore, a kinematic pair adjacency matrix M_{KPA} is constructed to describe the PM in this section, as shown in formula (1). The information contained in the matrix M_{KPA} includes the number of components, the number of kinematic pairs, the type of kinematic pairs, the spatial position relationship of kinematic pairs, and the connection relationship between components and kinematic pairs, etc. The configuration characteristics of PM are expressed more comprehensively in the matrix M_{KPA}.

$$
M_{\mathrm{KPA}} = \begin{bmatrix}
L_1 & {}^{C2}_{pq}J^{12} & {}^{C3}_{pq}J^{13} & \cdots & {}^{Ci}_{pq}J^{1i} & \cdots & {}^{C(n-1)}_{pq}J^{1,n-1} & {}^{Cn}_{pq}J^{1,n} \\
a_{21} & L_2 & {}^{C3}_{pq}J^{23} & \cdots & {}^{Ci}_{pq}J^{2i} & \cdots & {}^{C(n-1)}_{pq}J^{2,n-1} & {}^{Cn}_{pq}J^{2,n} \\
a_{31} & a_{32} & L_3 & \ddots & \cdots & {}^{Cj}_{pq}J^{3j} & \cdots & \cdots \\
\vdots & \vdots & \ddots & \ddots & {}^{Ci}_{pq}J^{i-1,i} & \vdots & \vdots & \vdots \\
a_{i1} & a_{i2} & \cdots & a_{i,i-1} & L_i & {}^{C(i+1)}_{pq}J^{i,i+1} & \cdots & {}^{Cn}_{pq}J^{i,n} \\
\cdots & \cdots & a_{i+1,j} & \cdots & a_{i+1,i} & \ddots & \ddots & \cdots \\
a_{n-1,1} & a_{n-1,2} & \cdots & \cdots & \cdots & \ddots & L_{n-1} & {}^{Cn}_{pq}J^{n-1,n} \\
a_{n,1} & a_{n,2} & \cdots & \cdots & a_{n,i} & \cdots & a_{n,n-1} & L_n
\end{bmatrix}
\tag{1}
$$

where i is the row of the matrix and j is the column of the matrix, i, j, p, q represent the No. of the mechanism component, respectively, (i, j, p, $q = 1, 2, \ldots, n$); L_i represents the ith component of the mechanism according to the defined serial number; a_{ij} represents the connection relationship between various components of the mechanism; the left upper corner mark Cj represents the constraint type.

Through the constructed kinematic pair adjacency matrix M_{KPA} for the topological graph of PM, not only the degrees of freedom (DOF) of the mechanism can be obtained but also the diagram of the mechanism can be inversely described. Under the condition that only the matrix M_{KPA} of the mechanism is known, the information can be used to draw the mechanism diagram. These will be verified in the subsequent sections.

In the matrix of formula (1), the lower triangular element represents whether there is a connection relationship between various components of the mechanism, and its specific value is defined as follows:

$$
a_{ij} = \begin{cases}
0, & \text{No connection between the components } i \text{ and } j \\
1, & \text{There is a connection between the components } i \text{ and } j
\end{cases}
\tag{2}
$$

The diagonal element L_i represents the ith component of the mechanism according to the defined serial number. To express the information of the driving pair, the fixed platform, and the moving platform of mechanism, the diagonal element is defined and assigned as follows:

Table III. *Definition of position constraint type Cj for kinematic pair axis.*

Constraint type Cj	Element assignment	Type of axial constraint	Example
No	0	No positional relationship	No
a	1	The axes of adjacent kinematic pairs are parallel to each other	R‖R, R‖H, H‖H etc.
b	2	The axes of adjacent kinematic pairs are coaxial (coincident)	R|R, R|P, H|R, H|H, etc.
c	3	The axes of adjacent kinematic pairs intersect at the same point	(RRR), (RR), (R⊥R), etc.
d	4	The axes of adjacent kinematic pairs are perpendicular to each other	R⊥R, R⊥P, H⊥P, etc.
e	5	The prismatic pair is parallel to the same plane	◇ (P, P, P), etc.
f	6	The axes of the kinematic pair are in any direction	R-R, R-P, R-H, H-H, etc.

Table IV. *Definition of connection relationship.*

J^{ij}	Element assignment	DOF of kinematic pair	Meaning
No	0	0	There is no connection between i and j
R	1	1	The connection between i and j is a revolute pair
P	2	1	The connection between i and j is a prismatic pair
S	3	3	The connection between i and j is a spherical joint
U	4	2	The connection between i and j is a Hooke hinge
C	5	2	The connection between i and j is a cylindrical pair
H	6	1	The connection between i and j is a screw pair

$$L_i = a^{ii} = \begin{cases} 7, & \text{Component } i \text{ is the driving part} \\ 8, & \text{Component } i \text{ is the passive part} \\ 9, & \text{Component } i \text{ is the fixed platform} \\ 10, & \text{Component } i \text{ is the moving platform} \end{cases} \tag{3}$$

The upper triangular element $_{pq}^{Cj}J^{ij}$ indicates that the kinematic pair J is connected to the current component i and j, and the positional relationship between this axis of kinematic pair and the axis of connecting component p and q is the constraint type Cj. The left upper corner mark Cj represents whether there is a position connection between the axes of the kinematic pair in mechanisms. The lower left corner mark pq represents the axis of kinematic pair for connecting component p and q. There is a positional relationship between the axis of connecting component p and q and the axis of connecting component i and j. Among them, there are six kinds of positional relationships included in Cj, namely the axes in space are parallel, the axes are coaxial, the axes intersect at one point, the axes are perpendicular, the axes are parallel to the same plane, and the axes are in any direction [6, 9]. The specific definition and assignment are shown in Table III.

For the kinematic pair J^{ij} of the element $_{pq}^{Cj}J^{ij}$, it represents the connection relationship between the component i and j, and the specific definition and assignment are shown in Table IV.

In the kinematic pair adjacency matrix M_{KPA}, the expression elements $_{pq}^{Cj}J^{ij}$ for the axis position connection relationship of the kinematic pair are specifically described as follows:
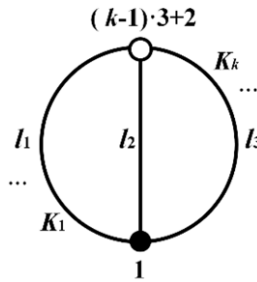
Figure 17. *Topological graph of spatial SPM (m = 3).*

R^{12} means that the component 1 and 2 are connected by the revolute pair. P^{34} means that the component 3 and 4 are connected by the prismatic pair. $_{23}^{a}R^{12}$ means that the component 1 and 2 are connected by the revolute pair, and the axis of the revolute pair is parallel to the axis of component 2 and 3 in space. $_{45}^{b}P^{34}$ means that the component 3 and 4 are connected by the prismatic pair, and the axis of the prismatic pair is coaxial (coincident) to the axis of component 4 and 5 in space. $_{67}^{f}S^{78}$ means that the component 7 and 8 are connected by the spherical pair, and the axis of the spherical pair is arbitrary with the axis of component 6 and 7 in space.

Moreover, the kinematic pair adjacency matrix M_{KPA} is analyzed. It has the following properties:

1. The lower triangular element a_{ij} in the matrix M_{KPA} described the connection relationship between components i and j. It is judged by the values of 0 and 1. If there is a connection relationship, the element value is 1; otherwise, it is 0.

2. The diagonal element L_i in the matrix M_{KPA} described the serial number and quantity of components in the mechanism. According to the size of the matrix M_{KPA} $n \times n$, it can be known that there are n components in the mechanism.

3. The upper triangular element $_{pq}^{Cj}J^{ij}$ in the matrix M_{KPA} described the types of kinematic pair between component i and j, and the spatial position relationships for the axis of kinematic pairs.

4. The DOF of the mechanism can be calculated through the information in the matrix M_{KPA}, such as the number of mechanism components, the number of kinematic pairs, and the type of kinematic pairs, etc.

5. The matrix M_{KPA} can be used to draw the spatial mechanism. With the help of the information of the number of mechanism components, the number of kinematic pairs, the type of kinematic pairs, and the spatial position relationship for the axis of kinematic pairs in the matrix, the topological graph for spatial mechanism can be drawn, and the diagram of mechanism can be further obtained.

6. The adjacency matrix of mechanism can be derived from the lower triangular element a_{ij} in the matrix M_{KPA}. The elements of the adjacency matrix are symmetrical about the diagonal. The diagonal elements are all 0, and the adjacency matrix belongs to the real symmetrical matrix.

4. Verification of the new topological expression method for spatial SPM

4.1. Verification and analysis based on the topological graph

To verify the corresponding consistency and uniqueness of the proposed new topological expression method in this paper with spatial SPM, the spatial SPM is obtained through the topological graph and kinematic pair adjacency matrix in this section. Here, the 3-RPS PM [25] is taken as an example for verification. In Section 3.2, different structural types of topological graph for spatial SPMs are obtained. When $m = 3$, as shown in Fig. 17, the topological graph of SPM with three identical branched structures in space is obtained based on Fig. 16.
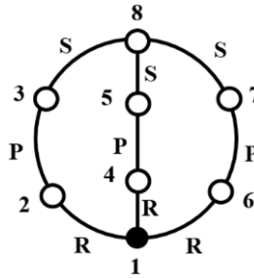
Figure 18. *Topological graph of 3-RPS PM.*

After determining the number of branches of the spatial SPM, if the connection relationship between the components is uncertain, many similar topological relationships of configurations can be generated. For example, the 3-RPS, 3-PRS, 3-SPR, 3-RRC, 3-RRPR, and other three-branch SPMs can be represented by Fig. 18. Hence, the kinematic pairs and the spatial position relationships of axes of each branch chain structure needed to be further clarified to determine the mechanism configuration. When the connection relationships between different components are given in the topological graph, a specific topological graph of SPM is generated. Here, the number of kinematic pairs in the topological graph Fig. 17 is set as $k = 3$, and the kinematic pairs of each branch chain adopt R, P, and S. Then, the topological relationship of the spatial SPM is formed, as shown in Fig. 18.

The 3-RPS PM is represented by the topological graph in Fig. 18. It is a typical representative of the 3-DOF PM and belongs to the spatial SPM. It can be seen from the topological graph that the mechanism is composed of three identical branch chains, a moving platform, and a fixed platform. Each branch chain contains three kinematic pairs: R, P, and S. The upper end is connected to the moving platform through the spherical pair, the lower end is connected to the fixed platform through the revolute pair, and the prismatic pair is in the middle of the branch chain.

According to the definition of the kinematic pair adjacency matrix M_{KPA} in Section 3.3, with the spatial position relationships of axes by $\{ -R \perp P - S - \}$ in each branch chain, the matrix M_{KPA} for the topological graph of 3-RPS PM can be obtained as follows:

$$M_{KPA} = \begin{bmatrix} L_1 & R^{12} & 0 & R^{14} & 0 & R^{16} & 0 & 0 \\ 1 & L_2 & {}^d_{12}P^{23} & 0 & 0 & 0 & 0 & 0 \\ 0 & 1 & L_3 & 0 & 0 & 0 & 0 & {}^f_{23}S^{38} \\ 1 & 0 & 0 & L_4 & {}^d_{14}P^{45} & 0 & 0 & 0 \\ 0 & 0 & 0 & 1 & L_5 & 0 & 0 & {}^f_{45}S^{58} \\ 1 & 0 & 0 & 0 & 0 & L_6 & {}^d_{16}P^{67} & 0 \\ 0 & 0 & 0 & 0 & 0 & 1 & L_7 & {}^f_{67}S^{78} \\ 0 & 0 & 1 & 0 & 1 & 0 & 1 & L_8 \end{bmatrix} \tag{4}$$

From the 8×8 square matrix of formula (4), it can be known that the PM is composed of eight components ($L_1, L_2, \ldots, L_8$), three revolute pairs (R), three prismatic pairs (P), and three spherical pairs (S). At the same time, information such as the connection relationship between each component, the type of kinematic pair, the spatial position relationship for the axis of kinematic pair, etc., are also expressed in the matrix. Among them, R^{12} means that the component 1 and 2 are connected by the revolute pair. ${}^d_{12}P^{23}$ means that the component 2 and 3 are connected by the prismatic pair, and its axis is in a d-type constraint relationship with the axis of revolute pair of component 1 and 2; that is, the two axes are perpendicular to each other. ${}^f_{23}S^{38}$ means that the component 3 and 8 are connected by spherical pair,

Table V. *Correspondence between the matrix M_{KPAU} and the branches of topological graph.*

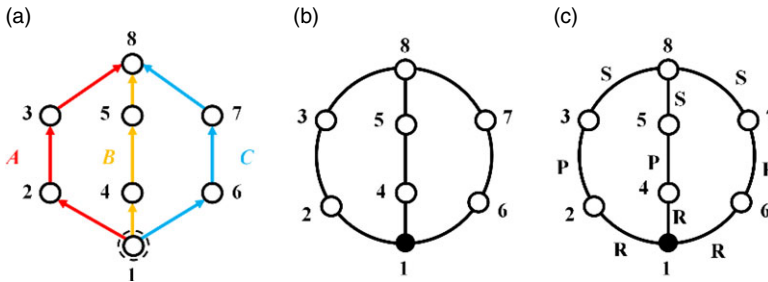| Branch	Kinematic pair elements	Single open chain (SOC)	Single branch chain
1	$R^{12}, {}_{12}^{d}P^{23}, {}_{23}^{f}S^{38}$	$\{-R^{12}\perp P^{23}-S^{38}-\}$	R-P-S
2	$R^{14}, {}_{14}^{d}P^{45}, {}_{45}^{f}S^{58}$	$\{-R^{14}\perp P^{45}-S^{58}-\}$	R-P-S
3	$R^{16}, {}_{16}^{d}P^{67}, {}_{67}^{f}S^{78}$	$\{-R^{16}\perp P^{67}-S^{78}-\}$	R-P-S

Figure 19. *The topological graph of 3-RPS PM obtained by M_{KPAU}. (a) The connection relationship. (b) Topological graph. (c) Topological graph of 3-RPS PM.*

and its axis is in the f-type constraint relationship with the axis of rotation pair of component 2 and 3, that is, the two axes intersect and can be in any orientation.

Combined with the information of the matrix M_{KPA}, according to the calculation formula of spatial degrees of freedom [26, 27], the DOF of this mechanism is obtained as follows:

$$M = 6(n - g - 1) + \sum_{i=1}^{g} f_i + \mu - \xi = 6 \times (8 - 9 - 1) + (1 \times 3 + 1 \times 3 + 3 \times 3) = 3$$

The above kinematic pair adjacency matrix M_{KPA} of the 3-RPS PM is further analyzed. By splitting the matrix M_{KPA}, the upper triangular matrix M_{KPAU} and the lower triangular matrix M_{KPAL} are obtained. The upper triangular matrix M_{KPAU} of the kinematic pair adjacency matrix is shown in formula (5).

$$M_{KPAU} = \begin{bmatrix} 0 & R^{12} & 0 & R^{14} & 0 & R^{16} & 0 & 0 \\ 0 & 0 & {}_{12}^{d}P^{23} & 0 & 0 & 0 & 0 & 0 \\ 0 & 0 & 0 & 0 & 0 & 0 & 0 & {}_{23}^{f}S^{38} \\ 0 & 0 & 0 & 0 & {}_{14}^{d}P^{45} & 0 & 0 & 0 \\ 0 & 0 & 0 & 0 & 0 & 0 & 0 & {}_{45}^{f}S^{58} \\ 0 & 0 & 0 & 0 & 0 & 0 & {}_{16}^{d}P^{67} & 0 \\ 0 & 0 & 0 & 0 & 0 & 0 & 0 & {}_{67}^{f}S^{78} \\ 0 & 0 & 0 & 0 & 0 & 0 & 0 & 0 \end{bmatrix} \quad (5)$$

From the element information of the matrix M_{KPAU}, the connection order and branch chain loop between components are obtained, as shown in Table V.

Further, the information in the matrix M_{KPAU} can be used to obtain the connection relationship of components, as shown in Fig. 19(a). Starting from component 1 to get the topological relationship diagram, as shown in Fig. 19(b). Then, combining the kinematic pair information from the matrix M_{KPAU} and expressing it to form the topological graph of SPM, as shown in Fig. 19(c).
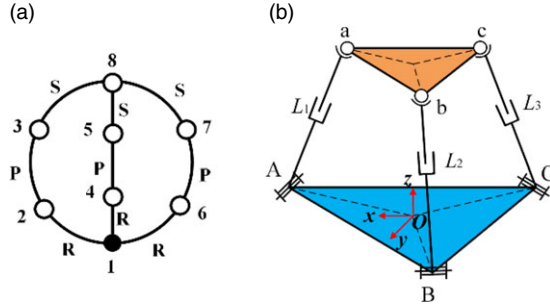
Figure 20. *Topological graph and corresponding 3-RPS PM. (a) Topological graph. (b) 3-RPS parallel mechanism.*

To sum up, by combining the topological graph of the 3-RPS PM with the information expressed by the kinematic pair adjacency matrix M_{KPA} of formula (4), the spatial symmetrical 3-RPS PM is uniquely determined. Then, the topological graph of mechanism is evolved from plane to space, and the corresponding spatial 3-RPS PM is obtained, as shown in Fig. 20.

In addition, based on the kinematic pair adjacency matrix M_{KPA}, the lower triangular matrix M_{KPAL} is obtained, as shown in formula (6).

$$M_{\mathrm{KPAL}} = \begin{bmatrix} 0 & 0 & 0 & 0 & 0 & 0 & 0 & 0 \\ 1 & 0 & 0 & 0 & 0 & 0 & 0 & 0 \\ 0 & 1 & 0 & 0 & 0 & 0 & 0 & 0 \\ 1 & 0 & 0 & 0 & 0 & 0 & 0 & 0 \\ 0 & 0 & 0 & 1 & 0 & 0 & 0 & 0 \\ 1 & 0 & 0 & 0 & 0 & 0 & 0 & 0 \\ 0 & 0 & 0 & 0 & 0 & 1 & 0 & 0 \\ 0 & 0 & 1 & 0 & 1 & 0 & 1 & 0 \end{bmatrix} \tag{6}$$

Then, the adjacency matrix M_{A} is further derived from the lower triangular matrix M_{KPAL}, as shown in formula (7). The matrix M_{A} is an 8×8 square matrix, so the corresponding mechanism has eight components. The connection relationship between each component is also expressed. Among them, the diagonal elements are all 0, the elements are symmetrical about the diagonal, and the matrix M_{A} belongs to a real symmetrical matrix.

$$M_{\mathrm{A}} = \begin{bmatrix} 0 & 1 & 0 & 1 & 0 & 1 & 0 & 0 \\ 1 & 0 & 1 & 0 & 0 & 0 & 0 & 0 \\ 0 & 1 & 0 & 0 & 0 & 0 & 0 & 1 \\ 1 & 0 & 0 & 0 & 1 & 0 & 0 & 0 \\ 0 & 0 & 0 & 1 & 0 & 0 & 0 & 1 \\ 1 & 0 & 0 & 0 & 0 & 0 & 1 & 0 \\ 0 & 0 & 0 & 0 & 0 & 1 & 0 & 1 \\ 0 & 0 & 1 & 0 & 1 & 0 & 1 & 0 \end{bmatrix} \tag{7}$$

After uniformly assigning values to the matrix elements, the corresponding matrix M_{KPA} for the topological graph of 3-RPS PM is obtained, as shown in formula (8).

$$M_{\mathrm{KPA}} = \begin{bmatrix} 9 & 1^{12} & 0 & 1^{14} & 0 & 1^{16} & 0 & 0 \\ 1 & 7 & {}_{12}^{4}2^{23} & 0 & 0 & 0 & 0 & 0 \\ 0 & 1 & 8 & 0 & 0 & 0 & 0 & {}_{23}^{6}3^{38} \\ 1 & 0 & 0 & 7 & {}_{14}^{4}2^{45} & 0 & 0 & 0 \\ 0 & 0 & 0 & 1 & 8 & 0 & 0 & {}_{45}^{6}3^{58} \\ 1 & 0 & 0 & 0 & 0 & 7 & {}_{16}^{4}2^{67} & 0 \\ 0 & 0 & 0 & 0 & 0 & 1 & 8 & {}_{67}^{6}3^{78} \\ 0 & 0 & 1 & 0 & 1 & 0 & 1 & 10 \end{bmatrix} \tag{8}$$

To facilitate computer processing, according to the upper triangular matrix M_{KPAU} of formula (5), the symmetry of the matrix about the diagonal elements is used to obtain the adjacency matrix M_{A}. After uniformly assigning values to the matrix M_{A} and simplifying the expression information, the numerical matrix M_{D} is derived, as shown in formula (9).

To facilitate computer processing, according to the upper triangular matrix M_{KPAU} of formula (5), by taking advantage of the symmetry of the matrix M_{KPAU} about the diagonal elements, that is, making the matrix elements $a_{ij} = a_{ji}, (i \neq j)$, and then symmetrizing the upper triangular matrix elements and simplifying the information of the upper and lower corner markers of the matrix elements, the matrix M_{D} based entirely on the numerical expression is derived, as shown in formula (9).

$$M_{\mathrm{D}} = \begin{bmatrix} 9 & 1 & 0 & 1 & 0 & 1 & 0 & 0 \\ 1 & 7 & 2 & 0 & 0 & 0 & 0 & 0 \\ 0 & 2 & 8 & 0 & 0 & 0 & 0 & 3 \\ 1 & 0 & 0 & 7 & 2 & 0 & 0 & 0 \\ 0 & 0 & 0 & 2 & 8 & 0 & 0 & 3 \\ 1 & 0 & 0 & 0 & 0 & 7 & 2 & 0 \\ 0 & 0 & 0 & 0 & 0 & 2 & 8 & 3 \\ 0 & 0 & 3 & 0 & 3 & 0 & 3 & 10 \end{bmatrix} \tag{9}$$

where i is the row of the matrix and j is the column of the matrix, i and j represent the No. of the mechanism component, respectively, ($i = 1, 2, \ldots, 8; j = 1, 2, \ldots, 8$). The diagonal values 7, 8, 9, 10 represent that the ith component of the mechanism is the driving component, the passive component, the fixed platform, and the moving platform, respectively; the values 1, 2, 3 in the matrix represent that the components i and j are connected with each other through the revolute pair R, the prismatic pair P, and the spherical pair S, respectively; the value 0 in the matrix represents that there is no topological connection between the components i and j.

Hence, based on the numerical matrix M_{D}, the configuration of PM can be designed and analyzed with the help of the computer programming.

4.2. Verification and analysis based on the spatial SPM

To verify the corresponding consistency of the spatial SPM with the new topological expression method proposed in this paper, the 3-RRC PM is taken as an example to obtain its corresponding topological graph and kinematic pair adjacency matrix in this section.

The 3-RRC PM is a spatial SPM, and it can realize three-dimensional translational motion, as shown in Fig. 21. From the diagram of the 3-RRC PM, it consists of three identical branches, a moving platform and a fixed platform, with a total of eight components. Each branch chain includes three kinematic pairs: R, R, and C, and the axes of these kinematic pairs are parallel to each other. The lower end of each branch chain is connected to the fixed platform through the first revolute pair, and the upper end is connected to the moving platform through the cylindrical pair. Based on the above information, the topological graph of 3-RRC PM can be further obtained, as shown in Fig. 22.
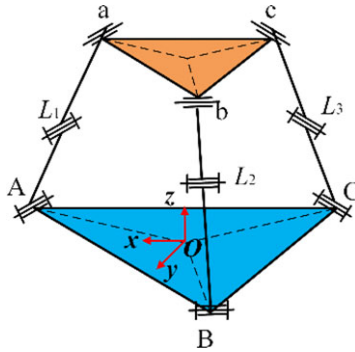
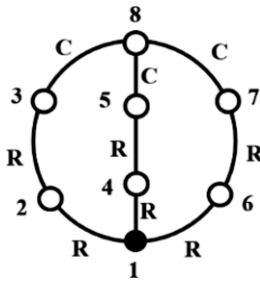**Figure 21.** *The diagram of 3-RRC PM.*

Figure 22. *The topological graph of 3-RRC PM.*

Combining the information in the diagram with the topological graph of 3-RRC PM, the kinematic pair adjacency matrix M_{KPA} for the topological graph of 3-RRC PM can be obtained, as shown in formula (10).

$$
M_{KPA} =
\begin{bmatrix}
L_1 & R^{12} & 0 & R^{14} & 0 & R^{16} & 0 & 0 \\
1 & L_2 & {}^a_{12}R^{23} & 0 & 0 & 0 & 0 & 0 \\
0 & 1 & L_3 & 0 & 0 & 0 & 0 & {}^a_{23}C^{38} \\
1 & 0 & 0 & L_4 & {}^a_{14}R^{45} & 0 & 0 & 0 \\
0 & 0 & 0 & 1 & L_5 & 0 & 0 & {}^a_{45}C^{58} \\
1 & 0 & 0 & 0 & 0 & L_6 & {}^a_{16}R^{67} & 0 \\
0 & 0 & 0 & 0 & 0 & 1 & L_7 & {}^a_{67}C^{78} \\
0 & 0 & 1 & 0 & 1 & 0 & 1 & L_8
\end{bmatrix}
\tag{10}
$$

After the same assignment, the corresponding kinematic pair adjacency matrix M_{KPA} and the numerical adjacency matrix M_D are obtained, as shown in formulas (11) and (12).

$$
M_{KPA} =
\begin{bmatrix}
9 & 1^{12} & 0 & 1^{14} & 0 & 1^{16} & 0 & 0 \\
1 & 7 & {}^1_{12}1^{23} & 0 & 0 & 0 & 0 & 0 \\
0 & 1 & 8 & 0 & 0 & 0 & 0 & {}^1_{23}5^{38} \\
1 & 0 & 0 & 7 & {}^1_{14}1^{45} & 0 & 0 & 0 \\
0 & 0 & 0 & 1 & 8 & 0 & 0 & {}^1_{45}5^{58} \\
1 & 0 & 0 & 0 & 0 & 7 & {}^1_{16}1^{67} & 0 \\
0 & 0 & 0 & 0 & 0 & 1 & 8 & {}^1_{67}5^{78} \\
0 & 0 & 1 & 0 & 1 & 0 & 1 & 10
\end{bmatrix}
\tag{11}
$$

(a)
Adjacency matrix topology mapping relationship

(b)
Upper triangular matrix topology mapping relationship

(c)
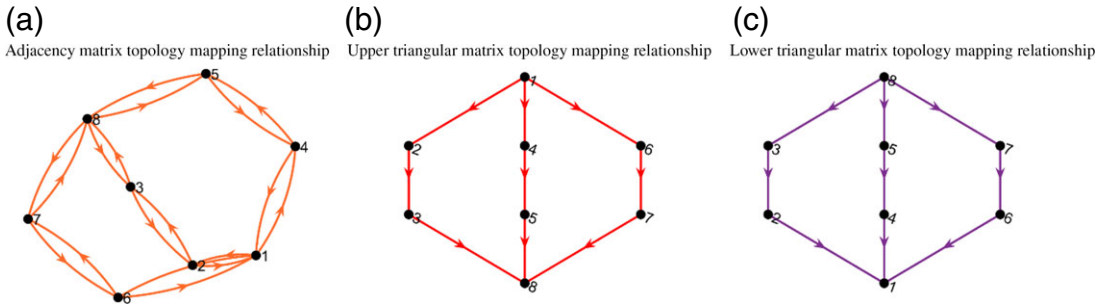Lower triangular matrix topology mapping relationship

Figure 23. *Topological traversal model of the adjacency matrix for 3-DOF SPM: (a) Adjacency matrix. (b) Upper triangular adjacency matrix. (c) Lower triangular adjacency matrix.*

$$M_{\mathrm{D}} = \begin{bmatrix} 9 & 1 & 0 & 1 & 0 & 1 & 0 & 0 \\ 1 & 7 & 1 & 0 & 0 & 0 & 0 & 0 \\ 0 & 1 & 8 & 0 & 0 & 0 & 0 & 5 \\ 1 & 0 & 0 & 7 & 1 & 0 & 0 & 0 \\ 0 & 0 & 0 & 1 & 8 & 0 & 0 & 5 \\ 1 & 0 & 0 & 0 & 0 & 7 & 1 & 0 \\ 0 & 0 & 0 & 0 & 0 & 1 & 8 & 5 \\ 0 & 0 & 5 & 0 & 5 & 0 & 5 & 10 \end{bmatrix} \tag{12}$$

So far, through the diagram of 3-RRC PM, the 3-RRC PM is transformed into the expression of the planar topological relationship, and the corresponding topological graph and kinematic pair adjacency matrix are established. By using the kinematic pair adjacency matrix, various connection relationships between components in the topological graph of the 3-RRC PM are described in detail. The corresponding consistency of the 3-RRC PM with the proposed new topological expression method is verified. At the same time, combined with the numerical matrix, it will be convenient to use for digital and automated design of the SPM configuration.

5. Example for digital and automated design based on topological graph

To obtain all the parallel mechanisms that meet the requirements and to facilitate computer processing, it is necessary to generate the adjacency matrix based on the topological graph of the SPM. Then, the topological traversal model of the mechanism can be established by computer programming, and using constraints to remove isomorphic structures, all targeted mechanisms will be obtained.

Taking the 3-DOF SPM as an example, by creating the topological traversal model as shown in Fig. 23 to get all parallel mechanisms. This topological traversal model represents all the three-branch SPMs with 3-DOF. During the topological traversal with computer programming, the following constraints need to be satisfied: (1) the traversal does not change the degrees of freedom; (2) the traversal does not change the number of branched chains; (3) the traversal does not change the symmetry; (4) the traversal can change the number and order of branched kinematic pairs.

For the topological traversal of the 3-DOF SPM, any basic configuration can be chosen. Here, taking the 3-RPS configuration in Section 4.1 as an example, the adjacency matrix MD is first derived from the mechanism topological graph, as shown in formula (9). Then, based on the adjacency matrix MD of the 3-RPS PM, the corresponding topological traversal model is obtained by computer programming transformation, as shown in Fig. 24.
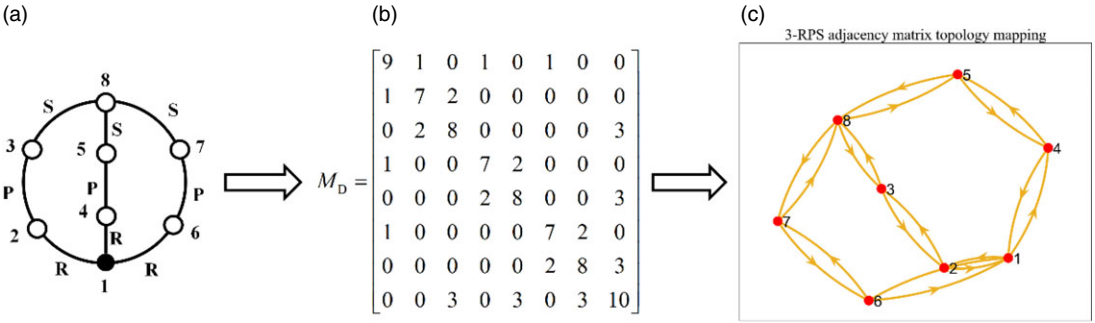
Figure 24. *Adjacency matrix and traversal model of the 3-RPS PM: (a) Topological graph of 3-RPS SPM. (b) Adjacency matrix MD. (c) Topological traversal model.*
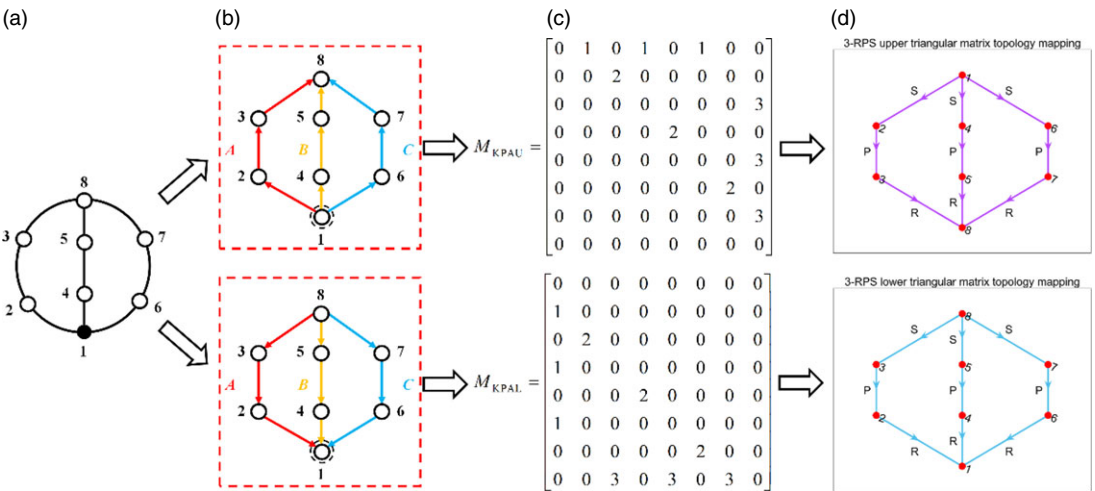

Figure 25. *Triangular matrix of 3-RPS and corresponding topological traversal model: (a) Topological graph. (b) The connection relationship. (c) Matrix M_{KPAU}, M_{KPAL}. (d) Topological traversal model.*

As the adjacency matrix is a real symmetric matrix, it can be simplified by choosing its upper triangular matrix or lower triangular matrix for topological traversal. The topological traversal model is consistent with the topological connection relationship of the mechanism in Fig. 19 in Section 4.1, and its correspondence is shown in Fig. 25.

Then, the topological traversal algorithm will be designed to traverse all the topological models that satisfy the constraints proposed above. The preliminary design process of the topological traversal algorithm is shown in Fig. 26. Finally, the single-DOF kinematic pair combination is equivalent to replace the multi-DOF kinematic pair, and changing the kinematic pair arrangement order; then, the adjacency matrix of multiple mechanisms can be obtained, and further transforming the expression to generate all the target mechanism configurations.

The basic idea of the algorithm design is as follows:

1. Traverse all the kinematic pair types of each effective kinematic pair in the adjacency matrix M_D, and use the DOF calculation formula to filter the adjacency matrix M_D that satisfies the unchanging DOF;

2. Construct the configuration topology function of each effective kinematic pair in the adjacency matrix M_D, and transform the equivalent single-DOF kinematic pair combinations with multi-DOF kinematic pairs into each other to obtain all the adjacency matrices M_D;
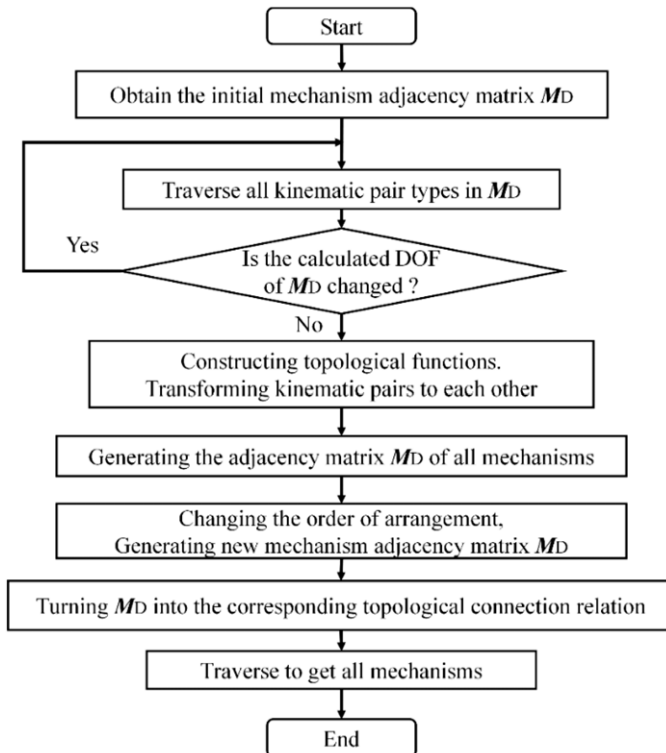
Figure 26. *Traversal algorithm process.*

3. For all the kinematic subsets in the adjacency matrix M_D generated in (2), change their arrangement order and generate the new adjacency matrix MD again;

4. Transform the adjacency matrix M_D obtained in (2) and (3) into the corresponding mechanism topological connection relations, and finally obtain all the mechanism configurations.

In conclusion, by designing the above traversal algorithm, all the 3-DOF SPM configurations satisfying the requirements will be further obtained, so as to achieve the goal of mechanism configuration synthesis. Since the complex research work is not yet completed, only basic ideas and methods of the research are given here. The next step of the research is to complete the algorithm design to obtain all the 3-DOF SPM configurations and realize the programmed design of the 3-DOF SPM configuration synthesis.

6. Conclusions

In this paper, the chemical molecular spatial structure (CMSS) is linked with the configuration of PM. From the perspective of CMSS, the evolution from spatial structure to planar topology is deduced and verified. The conclusions are as follows:

1. The planar topological graph of spatial regular tetrahedron molecular structure is obtained. With the topological evolution for the spatial structure of CH_4, the correlation of design between spatial structure and planar topological structure is verified.

2. A new topological expression method for spatial symmetrical parallel mechanism (SPM) is proposed. The topological graph of spatial SPM and the corresponding kinematic pair adjacency

matrix $\boldsymbol{M}_{\text{KPA}}$ are described and established, based on the evolution analysis with the topological relationship of the obtained spatial molecular structure.

3. The effectiveness and corresponding consistency of the new topological expression method for the spatial SPM are verified and analyzed, by taking the 3-RPS PM and 3-RRC PM as examples, respectively. The proposed new expression method paves the way for the subsequent digital and automated design and analysis of the PM configuration.

References

[1] T. Xu, Y. M. Chen and Z. F. Tian, "Structure-determinant properties: Three views of material genomic," *J. Huanggang Normal Univ.* **40**(6), 97–101 (2020).

[2] R. J. Gillespie and I. Hargittai, *The VSEPR Model of Molecular Geometry* (Courier Corporation, Chelmsford, MA, 2013).

[3] R. J. Gillespie and E. A. Robinson, "Models of molecular geometry," *Chem. Soc. Rev.* **34**(5), 396–407 (2005).

[4] J. G. Ferry, "Methane: Small molecule, big impact," *Science* **278**(5342), 1413–1414 (1997).

[5] H. F. Ding, Z. Huang and T. Zou, "Structure description of parallel mechanism," *J. Yanshan Univ.* **45**(1), 1–5 (2007).

[6] T. L. Yang, H. P. Shen, A. X. Liu and L. B. Hang, "Basic ideas and mathematical methods of mechanism topology theory-review of several original mechanism topology theories in a methodological perspective," *J. Mech. Eng.* **56**(3), 1–15 (2020).

[7] S. J. Li, D. L. Wang and J. S. Dai, "Topology of kinematic chains with loops and orientation of joints axes," *J. Mech. Eng.* **45**(6), 34–40 (2009).

[8] J. S. Dai and Q. X. Zhang, "Metamorphic mechanisms and their configuration models," *J. Mech. Eng.* **13**(3), 212–218 (2000).

[9] T. L. Yang, *Topology of Robotic Mechanisms* (Mechanical Industry Press, Beijing, 2004).

[10] G. Gogu, *Structural Synthesis of Parallel Robots (Part 2: Translational Topologies with Two and Three DoFs)* (Springer, Dordrecht, 2009).

[11] G. Gogu, *Structural Synthesis of Parallel Robots (Part 3: Topologies with Planar Motion of the Moving Platform)* (Springer, Dordrecht, 2010).

[12] Y. Lu and N. Ye, "Type synthesis of parallel mechanisms by utilizing sub-mechanisms and digital topological graphs," *Mech. Mach. Theory* **109**(3), 39–50 (2017).

[13] Y. Z. Li, Z. R. Wang, Y. G. Xu, J. S. Dai, Z. Zhao and Y.-A. Yao, "A deformable tetrahedron rolling mechanism (DTRM) based on URU branch," *Mech. Mach. Theory* **153**(11), 104000 (2020).

[14] F. F. Yang and Y. Chen, "One-DOF transformation between tetrahedron and truncated tetrahedron," *Mech. Mach. Theory* **121**(3), 169–183 (2018).

[15] H. H. Xiu, K. Y. Wang, T. Xu, G. W. Wei and L. Ren, "Synthesis and analysis of Fulleroid-like deployable Archimedean mechanisms based on an overconstrained eight-bar linkage," *Mech. Mach. Theory* **137**(7), 476–508 (2019).

[16] T. S. Mruthyunjaya, "Kinematic structure of mechanisms revisited," *Mech. Mach. Theory* **38**(4), 279–320 (2003).

[17] H. S. Yan, *Creative Design of Mechanical Devices* (Mechanical Industry Press, Beijing, 2002).

[18] J. K. Chu, R. Zhang and Y. H. Zou, *The Topological Structure Theory of Planar Mechanism and Its Application in Mechanism Innovation Design* (Science Press, Beijing, 2017).

[19] V. Henri, "The structure of the methane molecule," *Chem. Rev.* **4**(2), 189–201 (1927).

[20] Z. Y. Shen and X. Q. Wang, "Historical development of plane concepts and axioms," *J. Math. (China)* **57**(2), 6–11 (2018).

[21] H. F. Ding and Z. Huang, "Automatic creation of topological graphs and the characteristic representations of kinematic chains based on the loop characteristics," *J. Mech. Eng.* **43**(11), 40–43 (2007).

[22] H. F. Ding, Z. Huang, L. G. Liu and Y. Cao, "Computerized sketching of topological graphs of kinematic chains and obtaining of characteristic representations," *J. Yanshan Univ.* **44**(1), 10–13 (2006).

[23] H. S. Yan and C. H. Kuo, "Topological representations and characteristics of variable kinematic joints," *ASME J. Mech. Des.* **128**(2), 384–391 (2006).

[24] K. C. Lu, *Graph Theory and Its Applications* (Tsinghua University Press, Beijing, 1984).

[25] K. H. Hunt, "Structural kinematics of in-parallel-actuated robot-arms," *ASME J. Mech. Des.* **105**(4), 705–712 (1983).

[26] Z. Huang, Y. S. Zhao and T. S. Zhao, *Advanced Spatial Mechanism* (Higher Education Press, Beijing, 2006).

[27] Z. Huang, J. F. Liu and Y. W. Li, "150-year unified mobility formula issue," *J. Yanshan Univ.* **35**(1), 1–14 (2011).